

Boost decoding performance of finite geometry LDPC codes with deep learning tactics

Guangwen Li, Xiao Yu

Abstract—It was known a standard min-sum decoder can be unrolled as a neural network after weighting each edges. We adopt the similar decoding framework to seek a low-complexity and high-performance decoder for a class of finite geometry LDPC codes in short and moderate block lengths. It is elaborated on how to generate high-quality training data effectively, and the strong link is illustrated between training loss and the bit error rate of a neural decoder after tracing the evolution curves. Considering there exists a potential conflict between the neural networks and the error-correction decoders in terms of their objectives, the necessity of restraining the number of trainable parameters to ensure training convergence or reduce decoding complexity is highlighted. Consequently, for the referred LDPC codes, their rigorous algebraic structure promotes the feasibility of cutting down the number of trainable parameters even to only one, whereas incurring marginal performance loss in the simulation.

Index Terms—Deep learning, Neural networks, Belief propagation, Finite Geometry LDPC codes, Min-Sum, Training

I. INTRODUCTION

In modern telecommunication system, the error correction codes, as an indispensable ingredient, appears to combat unavoidable random noises in the communication channel via deliberately designed redundancy in encoding. Among them, the family of linear low-density parity-check codes (LDPC) [1] demonstrate prominent error correction capability by achieving near Shannon Limit asymptotically [2]. However, the accompanied iterative belief propagation (BP) decoders [3] require substantial computational resources, thus unbearable in some harsh applications. With the efforts to reduce decoding complexity effectively, min-sum (MS) and its variants normalized min-sum and offset min-sum (OMS) (NMS) [4], [5] were proposed as an approximation of the BP. Regretfully, the resulting performance loss is not negligible in most cases.

On the other hand, with the giant leap of computational power and rapid development of machine learning theory, various deep learning strategies were deployed broadly in the fields from traditional image processing [6], objection detection [7], face recognition [8] to more challenging tasks such as natural language processing [9] and autonomous driving [10] etc. Their success is commonly symbolized with a state-of-the-art performance, even surpassing human-level in some metrics such as accuracy or response time [11], [12].

Many attempts have recently been explored to combine deep learning methods with low-complexity MS variants. To

G.Li is with the College of Information & Electronics, Shandong Technology and Business University, Yantai, China e-mail: lgwa@sdu.edu.cn

X.Yu is with the Department of Physical Sports, Binzhou Medical University, Yantai, China e-mail: yuxiao@bjmu.edu.cn

overcome in code space the obstacle, known as curse of dimensionality [13], the authors in [14]–[19] proposed to optimize trainable weights or offsets to obtain neural normalized min-sum (NNMS) or neural offset min-sum (NOMS) decoders respectively, after unrolling the original min-sum schemes with respect to the Tanner graph of a code into typical neural networks such as convolutional neural network (CNN) or recurrent neural network (RNN). It was verified that such approaches can achieve near maximum a posteriori (MAP) decoding performance for linear channel codes such as BCH codes and short Gallager LDPC codes [20]. Furthermore, for a class of protograph-based 5G LDPC codes, whose structure is quasi cyclic, [21], [22] explored to apply machine learning techniques with fully sharing edge weights for long block codes. Besides that, for a class of irregular LDPC codes, it was proposed in [23] to assign and share weights in terms of its degree distribution for the NNMS decoder.

In this paper, we stick to the framework of NNMS and elaborate on its training process. That is, how to generate effectively a quality training data to enhance decoder performance is discussed in detail, and we also take a close look at the strong link between training loss and decoding metrics such as bit error rate(BER) or frame error rate (FER). For a class of finite-geometry LDPC (FG-LDPC) codes [24], the unique characteristic of encoding in linear time makes it advantageous over LDPC codes with other constructions. Our target is to seek a low complexity decoder, with the framework of NNMS, for such codes with short and moderate block lengths. Unfortunately, it is found the concurrence of deep learning methods and iterative MS variants may conflict. The goal of MS variants is in search of a valid codeword iteratively, whereas that of deep learning is a local minima via updating parameters consecutively. Although there exists a strong positive correlation between loss and BER, it is verified excessive parameters may deter the NNMS, a compound decoder of neural network and MS variants, from converging to any codeword [19], especially for the FG-LDPC codes with rigorous algebraic structures. For another, a restricted number of parameters contributes to training convergence and reducing decoder complexity. It is demonstrated a NNMS decoder with only one adjustable parameter yields comparable performance with those decoders aided by much more parameters. Therefore, it is sensible to take the domain knowledge of code into consideration before diving into neural networks training.

The remainder of the paper is organized as follows. Section II presents the necessary background about LDPC decoding variants, as well as various NNMS or NOMS networking

structures. The motivation of our scheme is presented in Section III. The experimental results are discussed fully in Section IV. Section V concludes this work with some remarks and suggestions of further research directions.

II. BACKGROUND

For error correction codes, the redundancy added in channel encoding makes it possible to transmit information reliably over unreliable channels.

Assume each code bit $c_i, i = 1, 2, \dots, N$ is modulated with BPSK via $1 - 2c_i$, where N denotes code block length. Due to the disturbance by additive white Gaussian noise (AWGN) of zero mean and variance σ^2 , the log-likelihood ratio (LLR) of the i -th bit at channel output is given by

$$l_{v_i} = \log \left(\frac{p(y_i | c_i = 0)}{p(y_i | c_i = 1)} \right) = \frac{2y_i}{\sigma^2} \quad (1)$$

, where y_i is the i -th noisy signal. The LLR data can be described from the perspective of probability by means of sigmoid function. As a result, a large positive y_i hints high probability of symbol being 0 over 1, and the converse is equally true.

As a bipartite graph, a Tanner graph is derived from the parity check matrix \mathbf{H} which fully describes a code. It consists of two group of variable nodes and check nodes, the number of which are N and M respectively, as well as the edges connecting the inter-group members. Its structure pertains totally to the \mathbf{H} , where non-zero element '1' at row i column j denotes variable node i and check node j is connected with an edge.

Among many linear coding designs, the class of LDPC codes takes the lead in the arena for its outstanding performance where the standard BP is regarded as a competitive decoder, in the sense it is optimal under the condition of a tree-like Tanner graph without any cycles.

A. Standard BP and MS variants

To be self-contained, let us briefly describe BP decoding process. At the l -th iteration, on the i -th variable node side, the message sent to j check node is 2

$$x_{v_i \rightarrow c_j}^{(l)} = l_{v_i} + \sum_{\substack{c_p \rightarrow v_i \\ p \in \mathcal{C}(i)/j}} x_{c_p \rightarrow v_i}^{(l-1)} \quad (2)$$

Correspondingly, on the j -th check node side, the message to i -th variable node is 3

$$x_{c_j \rightarrow v_i}^{(l)} = 2 \tanh^{-1} \left(\prod_{\substack{v_q \rightarrow c_j \\ q \in \mathcal{V}(j)/i}} \tanh \left(\frac{x_{v_q \rightarrow c_j}^{(l-1)}}{2} \right) \right) \quad (3)$$

where $\mathcal{C}(i)/j$ denotes the neighboring check nodes of the i -th variable node excluding the j -th one, and $\mathcal{V}(j)/i$ the neighboring variable nodes of the j -th check node excluding the i -th one,

Above message updates between variable and check nodes occur on the edges of corresponding Tanner graph iteratively. Furthermore, at each iteration, hard decision is exerted on each bit with (4). If consequent binary vector $\hat{\mathbf{c}}$ satisfies the stopping criterion $\mathbf{H}\hat{\mathbf{c}} = \mathbf{0}$, the decoding terminates with a return of success. Otherwise, the process continues until the maximum number of iterations is met.

$$x_{v_i}^{(l)} = l_{v_i} + \sum_{\substack{c_p \rightarrow v_i \\ p \in \mathcal{C}(i)}} x_{c_p \rightarrow v_i}^{(l-1)} \quad (4)$$

$$x_{c_j \rightarrow v_i}^{(l)} = \left(\prod_{\substack{v_q \rightarrow c_j \\ q \in v(j)/i}} \text{sign} \left(x_{v_q \rightarrow c_j}^{(l-1)} \right) \right) \min_{\substack{v_q \rightarrow c_j \\ q \in v(j)/i}} \left| x_{v_q \rightarrow c_j}^{(l-1)} \right| \quad (5)$$

To circumvent expensive computation of hyperbolic tanh function, MS approximation (5) was proposed to substitute for (3), at the cost of some performance loss. What makes the MS more attractive is its characteristic of scale invariance [18], which is particularly applicable for the cases of channel noise with unknown variance. In comparison, the BP will suffer seriously in this situation.

Then NMS or OMS attempts to bridge performance gap between MS and BP decoders with a tuned correction factor or additive offset respectively, the effectiveness of which was fully investigated in literature.

B. Related work of neural implementations

After each iteration of NMS or OMS is unrolled into one hidden layer, the iterative decoder can be readily transformed into a trellis structure. To mitigate the adverse effects of dependent messages flow which degrades BP into a suboptimal decoder, NNMS and NOMS variants put weights or offsets on each message-passing edge as shown in 6 and 7, where $\alpha_{q,j}^{(l-1)}$ and $\beta_{q,j}^{(l-1)}$ denote the multiplicative weight and additive offset on the edge of variable node q to check node j at the $(l-1)$ -th iteration separately, and RL refers to the ReLu unit in deep learning.

$$x_{c_j \rightarrow v_i}^{(l)} = \left(\prod_{\substack{v_q \rightarrow c_j \\ q \in v(j)/i}} \text{sign} \left(x_{v_q \rightarrow c_j}^{(l-1)} \right) \right) \left(\alpha_{q,j}^{(l-1)} \min_{\substack{v_q \rightarrow c_j \\ q \in v(j)/i}} \left| x_{v_q \rightarrow c_j}^{(l-1)} \right| \right) \quad (6)$$

$$x_{c_j \rightarrow v_i}^{(l)} = \left(\prod_{\substack{v_q \rightarrow c_j \\ q \in v(j)/i}} \text{sign} \left(x_{v_q \rightarrow c_j}^{(l-1)} \right) \right) RL \left(\min_{\substack{v_q \rightarrow c_j \\ q \in v(j)/i}} \left| x_{v_q \rightarrow c_j}^{(l-1)} \right| - \beta_{q,j}^{(l-1)} \right) \quad (7)$$

Optionally, multiplicative parameters $w^{(l)}$ and γ^l can be imposed on each term of the right hand side of 2 or 4 to weight each other. Till now, the trellis structures are adapted into a class of neural networks where the size of trainable parameters is adjustable. For the purpose of illustration, the deep neural network architecture of NNMS is depicted as Fig. 1,

In training phase, the neural decoders starts off with a data batch feeding, then outputs its loss, followed by updating

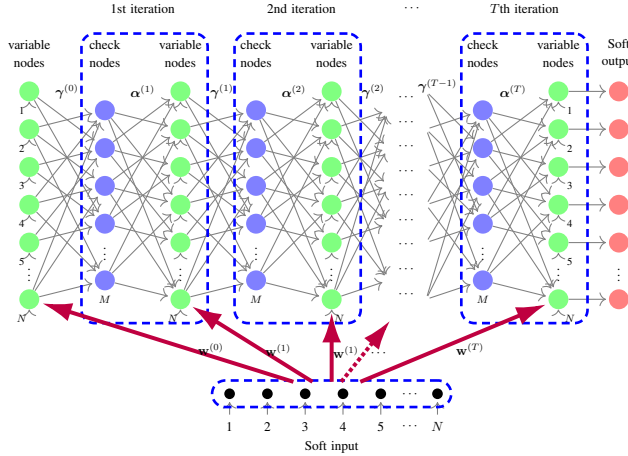


Fig. 1. A fully fledged NNMS framework in which the number of parameters $\alpha^{(l)}, \gamma^{(l)}, \mathbf{w}^{(l)}$, as well as the maximum number of iterations T , can be tailored to meet the need of applications, and N and M the number of and variable nodes and check nodes respectively.

all trainable parameters with back propagation rule. More feedings, more updates. The training continues until the loss function halts its long decline. In inference or test phase, the trained NNMS can effectively enhance decoding performance.

III. MOTIVATION OF OUR SCHEME

Totally, four classes of FG LDPC codes can be constructed based on the lines and points of Euclidean and projective geometries over finite fields [24]. As a family of cyclic or quasi-cyclic codes, it is feasible to encode messages with linear feedback shift registers, which makes such codes design fascinating in practice.

On the other hand, as a class of regular LDPC codes, the check matrix of FG-LDPC codes is square and both its row and column weights are much heavier than the counterpart with other constructions, which make any BP implementation computational demanding.

To alleviate it, we resort to the existing NNMS framework mentioned in Section II for decoding task, in the purpose of pursuing a better tradeoff between decoding performance and complexity. Specifically, two subjects are worth digging in training phase. one is how to generate a volume of training data purposefully to obtain a more robust neural decoder with competitive decoding performance. For another, as a compound of traditional MS and neural network, a neural decoder works via exchanging weighted messages through the interconnected edges marked in the parity check matrix H of a code. In essence, the MS concerns lowering FER or BER of transmitted codewords, while the neural network mind reducing loss via constantly tuning parameters. Thus it involves coordinating two competing parts for a common decoding task. How to avoid the potential interference which may lead to a failure of training convergence due to the goal discrepancy mentioned? In our view, the MS component should play a dominant role in updating and distributing messages, whereas the group of trainable parameters, standing

for the neural network component, is auxiliary by weighting those messages. To fulfill it, in the context of FG-LDPC codes, managing the number of trainable parameters is the key to a solution.

IV. EXPERIMENTAL RESULTS

Limited by space, two high rate FG-LDPC codes are discussed herein, constructed in accordance with the procedures in [24]. The type-I 2-D projective geometry LDPC code (273,191), belonging to the subclass of regular codes, has a squared circular parity-check matrix with row or column weight 17. While the type-I Euclidean geometry LDPC code (1023,781) holds a squared quasi-circular H , whose weight is 32. Although there exists an abundance of short cycles of length 6 in the parity-check matrix, its highly row redundancy assists such a FG-LDPC code to outperform its counterparts such as classical Gallager LDPC codes [24].

A. Training phase

For the ensemble of NNMS decoders, it is sufficiently clear to distinguish them from each other by the number and locations of trainable parameters. In the following, 'SNNMS' refers to the neural decoder with a shared weight at the check nodes side of each iteration, that is, $\gamma^{(l)} = \gamma^{(l)}$ as shown in Fig. 1. Likewise, 'UNNMS' is the one with a single parameter at the check nodes side across all iterations, or $\gamma^{(l)} = \gamma$. In the context of FG-LDPC codes, the left decoders in the ensemble are confirmed to be less competitive for achieving marginal performance improvement in the simulation over the mentioned ones, at the cost of much more trainable parameters. So they are safely omitted in the following plots of performance comparison.

After setting the maximum number of iterations T , each of which is equivalent to one hidden layer, we perform model training and testing using TensorFlow2.x on Colab or Kaggle cloud platforms.¹

1) *Definition of loss function*: Before start training, we have to select a viable loss function among many ones off the shelf, when turning to a stochastic gradient descent (SGD) method for optimizing target parameters. In our application, the hybrid version of cross entropy and mean squared error (MSE) is applied, as listed below,

$$\ell(c, \hat{c}) = \frac{\rho}{NT} \sum_{j=1}^T \sum_{i=1}^N \left(p(c_i = 0) \log \frac{1}{p(\hat{c}_i^j = 0)} + p(c_i = 1) \log \frac{1}{p(\hat{c}_i^j = 1)} \right) + \frac{100(1-\rho)}{N} \sum_{j=1}^T \left(p(c_i = 0)p^2(\hat{c}_i^j = 0) + p(c_i = 1)(p(\hat{c}_i^j = 1) - 1)^2 \right) \quad (8)$$

where ρ is a weight factor, $p(\hat{c}_i^j = 0)$ the probability of hard-decision of the i -th bit being '0' at the j -th iteration, constant 100 a scaling factor.

The cross entropy term in 8, measures the difference of density distributions of the estimated codeword bits and the ground truth, where a 'multiloss' approach [25], via averaging the cross entropy of all T iterations, is taken to yield a more

¹Related source code will soon be open in github website after documenting well

stable outcome. And the MSE term measures deviation of reliability of hard-decision from the original label on average. Such composition of a loss function, plus sufficiently large size of minibatch, is verified to guarantee the SGD method to generate a consistent gradient in updating target parameters, thus reducing the risk of divergence caused by parameter oscillation.

2) *Choice of training data*: Furthermore, with the assumption of all-zeros codewords sending, 8 reduces to

$$\ell(\mathbf{c}, \hat{\mathbf{c}}) = \frac{\rho}{NT} \sum_{j=1}^T \sum_{i=1}^N \log \frac{1}{p(\hat{c}_i^T = 0)} + \frac{100(1-\rho)}{N} \sum_{j=1}^N p^2(\hat{c}_i^T = 0) \quad (9)$$

In contrast to other deep learning applications where training data are rare or hard to acquire, it is effortless to obtain volumes of data at our discretion to feed a decoder, since the process of transmitting codewords through communication channel with AWGN noise added is fulfilled completely via simulation.

Notably, the assumption of only all-zeros codeword transmitted, has no impact on the validness of inferences generalized to the cases of non-zero codeword, besides simplifying training process. This unique property, attributed to satisfying the message passing symmetry conditions [26], is held by the ensemble of neural decoders. As a result, the calculation of bit error rate (BER) or frame error rate (FER) of a decoder is independent of the content of encoded codewords.

For both codes, each minibatch comprises of samples drawn equally from S signal-to-noise(SNR) points which are evenly spaced. For one thing, if the chosen SNR list is on the low side, strong noise will ruin the manoeuvre of learning the structure of neural decoder. Conversely, the objective of training deep learning network becomes obscure and inefficient, thus impeding the progress of coping with more noisy signals in test phase [13], [19].

In fact, we can derive exact density of such a blended minibatch, when aware of that the outcome variable Z with a mixture density, is a weight-sum of its component density of each normal random variable $Z_i = \frac{2}{\sigma_i^2} Y_i \sim N(\frac{2}{\sigma_i^2}, \frac{4}{\sigma_i^2})$, where Y_i is the channel output at the i -th SNR point. Thus in our scenario,

$$\begin{aligned} (SNR)_i &= \left(\frac{E_b}{N_0} \right)_i = 10 \log_{10} \frac{n}{2k\sigma_i^2}, \quad f(Z) = \sum_{i=1}^S w_i f_i(Z_i) = \frac{1}{S} \sum_{i=1}^S f_i(Z_i) \\ \Rightarrow E[Z] &= \mu = \sum_{i=1}^S w_i E[Z_i] = \sum_{i=1}^S \frac{2}{S\sigma_i^2}, D[Z] = \sigma^2 = \sum_{i=1}^S w_i (\sigma_i^2 + \mu_i^2) - \mu^2 \end{aligned} \quad (10)$$

For (1023,781) code, we obtain its mean $\mu = 6.096$ and variance $\sigma^2 = 12.232$ with 10. As shown in Fig. 2, it matches perfectly a Monte-Carlo sampling of the LLRs of input feeding a decoder. Interestingly, the density curve of a normal variable with the calculated (μ, σ^2) almost overlays that of the underlying mixture density, which suggests that a minibatch may be approximately generated instead by sampling a normal variable of appropriate parameters.

3) *Training settings*: All trainable parameters are initialized to be a identical 0.542 and thus push the softplus function $\log(1 + e^x)$ to generate for all weights the initial value of

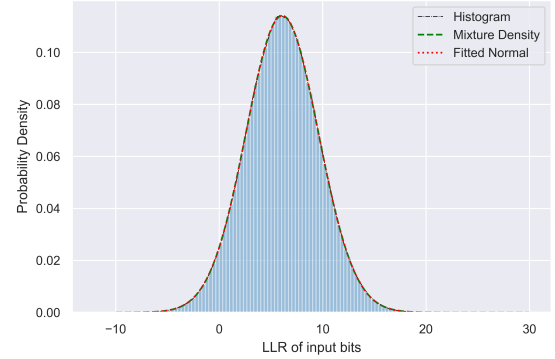


Fig. 2. Distribution of input' LLRs for (1023,781) code.

about 1, which poses the starting point of a neural decoder to be a standard MS in essence. Such a schedule can accelerate the training process to converge to a local optimum, compared with the routine normal distribution setting. Meanwhile, we lean on the Adam optimizer [27], among many SGD methods, to update those parameters repeatedly with an exponential decaying learning rate wherein initial rate is 0.002, decay rate 0.95 and decay steps 400.

For (273,191) and (1023,781) codes, as listed in Table I, the training settings are similar except with differed values assigned for some parameters.

TABLE I
TRAINING SETTINGS OF FG-LDPC CODES

Two Codes	SNR Range(dB)		Minibatch		# of epochs	T
	[min,max]	S	number	size		
(273,191)	[2.4,3.0]	4	4000	64	8	5
(1023,781)	[2.8,3.2]	5	600 ^a	80	8	10

^a Limited by upload speed and disk space

4) *Training process analysis*: It is often difficult to get the exact soft output distribution of a decoder analytically, thus we resort to the Monte-Carlo sampling to obtain the fitted density curve in Fig. 3. Apparently, the high density region concentrates on the positive clipped value 100, hinting most bits made correct choice of being '0' with high confidence.

For the instance of (1023,781) code with a SNNMS decoder, with the metrics of loss, BER and FER, Figs. 4-6 present the training evolution curves with or without smoothing.

As shown in Fig. 4, Initially, the loss is evaluated with 2.45 for the original input to the decoder, then degrading to 5.86 at early training stage. It works in concert with the fact that the performance of trained decoder over first several updates declines temporarily, compared even with the immediate hard-decision of channel output. However, with the proceeding of optimizing process, the loss drops to 0.67 finally. Meanwhile, the corresponding FER and BER drop almost at the same pace, which reveals the powerful strength of trainable network for us.

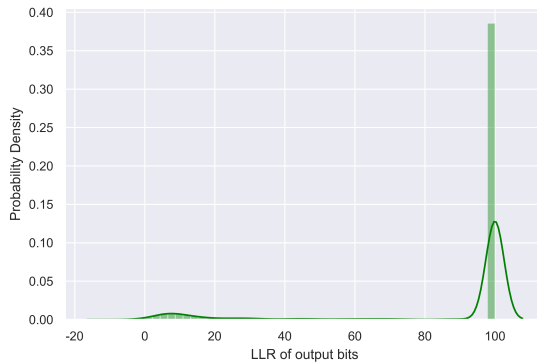


Fig. 3. Distribution of output LLRs for (1023,781) code.

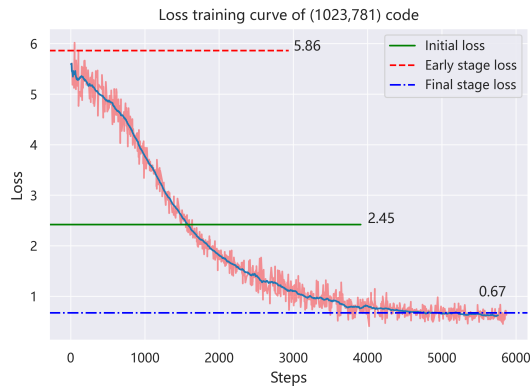


Fig. 4. Loss training curve of (1023,781) code.

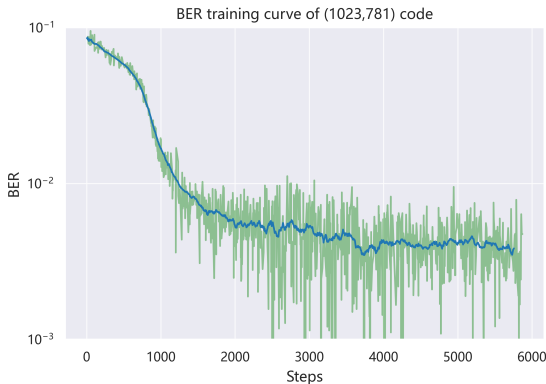


Fig. 5. BER training curve of (1023,781) code.

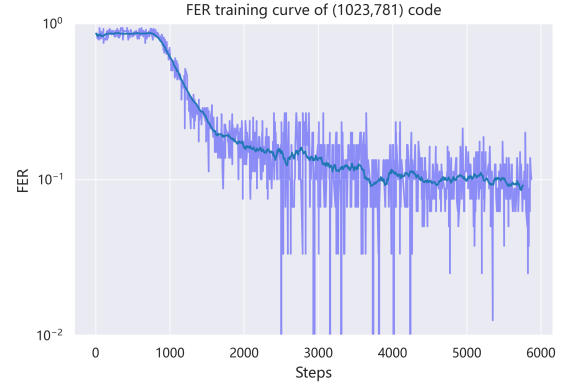


Fig. 6. FER training curve of (1023,781) code.

In particular, the immediate hard-decision or BER of decoder input is 0.04, approximated with

$$\int_0^{+\infty} \frac{1}{\sqrt{2\pi}\sigma} e^{-\frac{(x-\mu)^2}{2\sigma^2}} dx \quad (11)$$

where μ and σ^2 are obtained with 10. It is in accordance with the initial loss expressed with a horizontal line of height 2.45 in Fig. 4. Then at the moment where the loss curve drops to revisit this line, the accompanied BER is below 0.008 statistically. Consequently, identical loss value is mapped to multiple BERs, indicating that the training process plays the role of polarization, which cuts down largely the number of bits of weak confidence by virtue of message iterating, leading to a correct binary choice in most cases. The similar observation holds for FER metric as well.

5) *Training result analysis:* For (1023,781) code, we traced the transition of trainable parameters of the SNNMS decoder from beginning to end, and recorded some intermediate results in Table II.

TABLE II
EVOLUTATIONAL PARAMETERS AND RELATED METRICS FOR FG-LDPC
(1023,781) CODE

i-th step	weight list values	Loss	FER	BER
0	0.54/ 0.544/ 0.54/ 0.544/ 0.54/ 0.54 / 0.54 0.54 / 0.54	5.52	0.85	0.084
500	0.546 / 0.562 / 0.548 / 0.509 / 0.528 / 0.51 / 0.289 / -0.138 / -0.351 / -0.291	5.04	0.91	0.052
1600	0.569 / 0.523 / 0.418 / -0.074 / -1.021 / -1.435 / -1.13 / -0.978 / -0.986 / -0.98	2.79	0.23	0.0056
4400	0.307 / -0.051 / -0.974 / -1.748 / -1.177 / -1.06 / -1.034 / -1.028 / -1.065 / -1.126	1.43	0.11	0.0042
11999	-1.059 / -1.153 / -1.114 / -1.085 / -1.094 / -1.072 / -1.079 / -1.118 / -1.182 / -1.252	0.49	0.075	0.0035

Interestingly, in the course of training, it is observed the parameter list changed gradually from the initial state identically assigned 0.542, to the ending state all roughly equal to -1, attributed to the strength of neural network. Naturally, it reminds us to attempt the traditional NMS with the softplus function evaluated at the point of -1 as its correction factor, labelled as UNNMS as well in the following tests. As illustrated in the next subsection, such a simplification incurs no performance punishment. On the other hand, when we add into the neural NNMS more parameters $w^{(l)}$ to weight each bit of a codeword for the l -th iteration, the assigned identical initial

value 0.542 is hardly altered at the end of training, revealing that each bit is treated with no preference by the network. The similar observations also holds for (273,191) code.

B. Testing phase

The Monte-Carlo simulation is invoked again to accomplish the task of evaluating performance of a decoder. To minimize the variance of FER or BER estimate, at least 100 frame errors are required to be detected at each SNR point. For the neural decoders, $T = 5, 10$ are configured separately for (273,191) code and (1023,781) code.

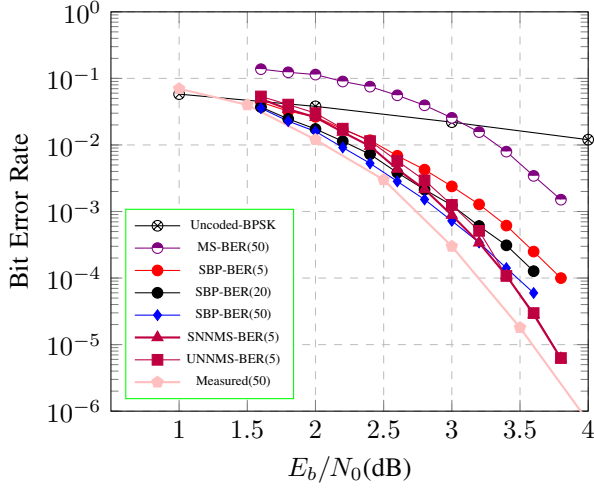


Fig. 7. BER comparison of various decoding schemes for (273,191) code

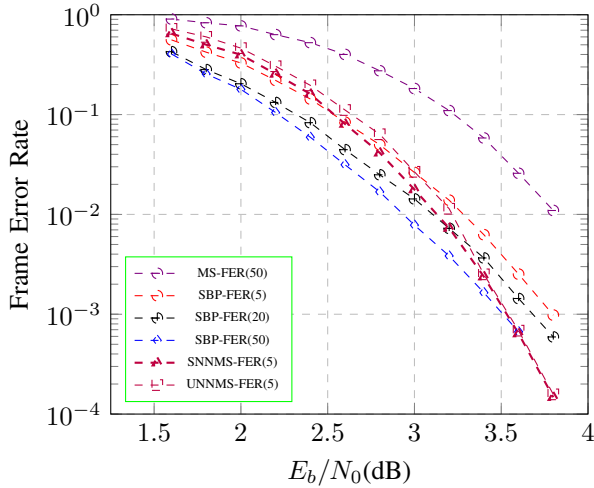


Fig. 8. FER comparison of various decoding schemes for (273,191) code

1) *Testing results analysis*: Fig. 7 shows BER curves of various decoders for (273,191) code. Notably, the Measured (50) denotes the plot is drawn with respect to the data obtained via measuring the relevant figure in [24] where its BP decoder was with $T = 50$, and the uncoded BPSK is presented as another benchmark.

It has to be declared firstly there exists an obvious performance discrepancy between the BP implementations of the measured and ours. Presumably it is attributed to two variations. For one thing, Considering the row weight of parity-check matrix for (273,191) code is 17, thus the required successive multiplication of up to 16 $tanh$ functions in updating the outgoing message of each check node is a challenge in terms of computation precision, and the situation is aggravated further in the scenario of all-zeros codeword sending in high SNR region where differed mandatory clippings may incur differed errors. For another, the message scheduling style in our BP implementation is a simple flooding in favor of parallel processing, while the measured one devoted itself to improving BER or FER via more advanced schedule such as the shuffled one [28] etc. To avoid ambiguity, our standard BP implementation is referred as 'SBP' hereinafter.

It is evident performance of MS is much less competitive, while that for SBP is augmented consistently when T increases from 5 to 50. Specifically, at the point $BER = 10^{-4}$, about 0.3dB gain is observed for the latter over the former. As far as the ensemble neural decoders are concerned, all members share the same performance, except with a marginal difference at most. More interestingly, the ensemble of SNNMS, UNNMS etc. with $T = 5$ iterations, all outperform SBP with $T = 50$ iterations in the waterfall region, even though their performance lags behind the Measured (50) within 0.2dB. The similar conclusions hold for FER comparison as well, as illustrated in Fig. 8. Thus the emergence of neural networks is an opportunity of designing a low-complexity, low-latency, and high-performance decoders.

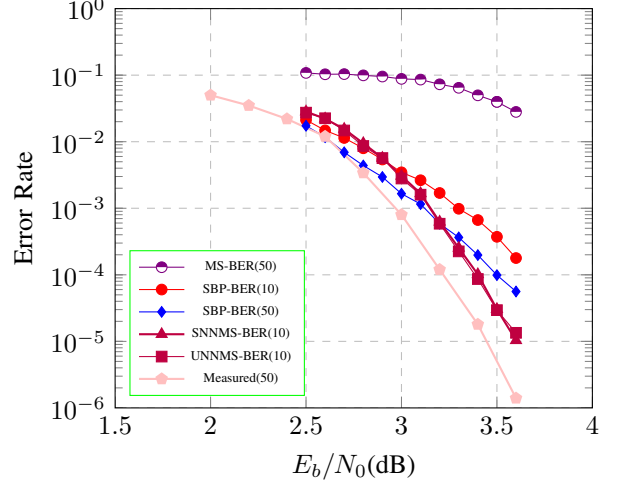


Fig. 9. BER comparison of various decoding schemes for (1023,781) code

The longer (1023,781) code has a row weight of 32 in its \mathbf{H} , and the gap between SBP and Measured (50) is widened to more than 0.3dB at the point of $BER=10^{-4}$ as seen in Fig. 9. Despite of that, the performance of neural ensemble with $T = 10$ closely follows Measured (50) within 0.2dB as well, as illustrated in both Figs. 9 and 10. Likewise, the other

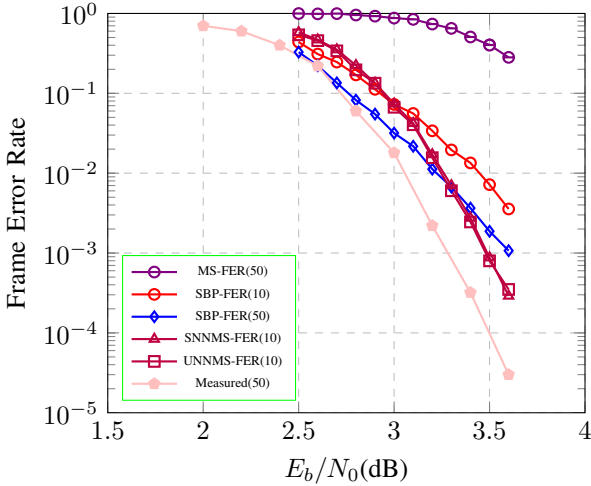


Fig. 10. FER comparison of various decoding schemes for (1023,781) code

observations for (273,191) code are largely preserved for this code as well.

Last but not the least, we have to rethink why each member of the neural ensemble on the premise of convergence in training phase, demonstrates similar decoding performance, regardless of the apparent variation in the number of trainable parameters. For instance, in terms of FER of Fig. 10, it is hard to distinguish in most SNR region the curves of SNNMS decoder with the UNNMS. How does that happen?

For the family of FG-LDPC codes, regarded as a manner of partly abandoning the distinct randomness owned by Gallager LDPC codes, they boast of rigorous algebraic circular or quasi-circular \mathbf{H} , thus the underlying encoding mechanism protects each bit or check of a codeword almost equally well, which makes the attempt of weighting each of them in vain. However, when a group consists of all bits and another one is filled with all checks, it is found effective to weight two groups with one adjustable parameter, leading to the prototype of UNNMS.

Therefore, it gives us some insights to re-examine the code structure so as to incorporate its domain knowledge into a neural decoder designing. A rush increase of the number of trainable parameters to pursue a powerful decoder may not boost decoding performance as expected, but left with some negative effects. For instance of (1023,781) code, a full-fledged NNMS decoder of 10 iterations is in need of a roughly million parameters to define the neural network under the assumption of no sharing, but the resultant gain is mean considering the superfluous increase of training load, decoder complexity and potential risk of divergence-prone, in comparison to the UNNMS with one tunable parameter.

C. Complexity analysis

Compared with standard BP with 50 iterations, the SNNMS and UNNMS implementation of both codes demand much fewer iterations of 5 and 10 separately, a hint of inbuilt advantage of low-latency.

Moreover, the neural variants call for some arithmetic additions and a few multiplications. While the BP takes at most a marginal lead in decoding, at the cost of expensive \tanh evaluations in addition to the handling of successive multiplications.

Surely the application of early stopping criterion can further reduce average decoding iterations of both the BP and the neural variants.

V. CONCLUSIONS AND FUTURE DIRECTIONS

we elaborate on how to generate quality data as the input to an ensemble of neural decoders in training. Then the roadmap of a training process is investigated in detail. For one thing, the positive correlation between loss and FER or BER metric was exposed after tracing the relevant evolution curves with tensorboard tool. For other, fully understanding the domain knowledge of a LDPC code before diving into designing its neural decoder is vital for an effective application of deep learning tactics, which is corroborated especially for the class of FG-LDPC codes underpinned by rigorous algebraic structures.

In summary, it is flexible to tailor the NNMS framework with a manageable number of parameters to bridge largely the performance gap between MS and BP decoders, at the cost of affordable overheads, thus achieving a better tradeoff between performance and complexity.

For the loss definition of 8, it is indicative of BER performance directly, whereas the effect of lowering FER is achieved via ensuring all bits belonging to a codeword are correctly decoded. To bypass this detour, it is helpful to refresh the loss definition by embracing a term related to enhancing FER. For instance, as pointed out in [29], it was valid to include a differentiable term pertained to decoding syndrome in the loss definition, which thus takes the associated FER into consideration as well when updating parameters in training. But its effectiveness remains to be checked in the case of FG-LDPC codes.

It is likely the ensemble of neural decoders are robust to minor parameter value shift, partly verified in the previous section. This feature can potentially be exploited to implement the arithmetic multiplication with a power of two, which is hardware friendly as far as the its implementation is concerned. Yet it has to be explored fully later.

Besides that, it is always worth trying some novel networking structures for the FG-LDPC codes to meet the demands of those challenging applications.

ACKNOWLEDGEMENT

The authors would like to thank Google corporation for providing the excellent computing platforms of Colab and Kaggle online, which make it possible to train and test our models freely.

REFERENCES

[1] R. Gallager, “Low-density parity-check codes,” *IRE Transactions on information theory*, vol. 8, pp. 21–28, 1962.

[2] D. J. C. MacKay and R. M. Neal, "Near shannon limit performance of low density parity check codes," *Electronics Letters*, vol. 32, p. 1645, 1996.

[3] M. P. C. Fossorier, M. Mihaljevic, and H. Imai, "Reduced complexity iterative decoding of low-density parity check codes based on belief propagation," *Ieee Transactions on Communications*, vol. 47, pp. 673–680, 1999.

[4] J. Zhao, F. Zarkeshvari, and A. H. Banihashemi, "On implementation of min-sum algorithm and its modifications for decoding low-density parity-check (ldpc) codes," *Ieee Transactions on Communications*, vol. 53, pp. 549–554, 2005.

[5] M. Jiang, C. Zhao, L. Zhang, and E. Xu, "Adaptive offset min-sum algorithm for low-density parity check codes," *Ieee Communications Letters*, vol. 10, pp. 483–485, 2006.

[6] M. I. Razzak, S. Naz, and A. Zaib, "Deep learning for medical image processing: Overview, challenges and the future," *Classification in BioApps*, pp. 323–350, 2018.

[7] R. J. Wang, X. Li, and C. X. Ling, "Pele: A real-time object detection system on mobile devices," *Advances in neural information processing systems*, vol. 31, 2018.

[8] G. Hu, Y. Yang, D. Yi, J. Kittler, W. Christmas, S. Z. Li, and T. Hospedales, "When face recognition meets with deep learning: an evaluation of convolutional neural networks for face recognition," in *Proceedings of the IEEE international conference on computer vision workshops*, 2015, pp. 142–150.

[9] T. Young, D. Hazarika, S. Poria, and E. Cambria, "Recent trends in deep learning based natural language processing," *ieee Computational intelligenCe magazine*, vol. 13, pp. 55–75, 2018.

[10] S. Grigorescu, B. Trasnea, T. Cocias, and G. Macesanu, "A survey of deep learning techniques for autonomous driving," *Journal of Field Robotics*, vol. 37, pp. 362–386, 2020.

[11] K. He, X. Zhang, S. Ren, and J. Sun, "Delving deep into rectifiers: Surpassing human-level performance on imagenet classification," in *Proceedings of the IEEE international conference on computer vision*, 2015, pp. 1026–1034.

[12] P. Mamoshina, A. Vieira, E. Putin, and A. Zhavoronkov, "Applications of deep learning in biomedicine," *Molecular pharmaceutics*, vol. 13, pp. 1445–1454, 2016.

[13] T. Gruber, S. Cammerer, J. Hoydis, and S. ten Brink, "On deep learning-based channel decoding," in *2017 51st Annual Conference on Information Sciences and Systems (CISS)*. IEEE, 2017, pp. 1–6.

[14] L. Lugosch and W. J. Gross, "Neural offset min-sum decoding," in *2017 IEEE International Symposium on Information Theory (ISIT)*. IEEE, 2017, pp. 1361–1365.

[15] E. Nachmani, E. Marciano, L. Lugosch, W. J. Gross, D. Burshtein, and Y. Be'ery, "Deep learning methods for improved decoding of linear codes," *IEEE Journal of Selected Topics in Signal Processing*, vol. 12, pp. 119–131, 2018.

[16] E. Nachmani, Y. Be'ery, and D. Burshtein, "Learning to decode linear codes using deep learning," in *2016 54th Annual Allerton Conference on Communication, Control, and Computing (Allerton)*. IEEE, 2016, pp. 341–346.

[17] F. Liang, C. Shen, and F. Wu, "An iterative bp-cnn architecture for channel decoding," *IEEE Journal of Selected Topics in Signal Processing*, vol. 12, pp. 144–159, 2018.

[18] L. P. Lugosch, *Learning algorithms for error correction*. McGill University (Canada), 2018.

[19] Q. Wang, S. Wang, H. Fang, L. Chen, L. Chen, and Y. Guo, "A model-driven deep learning method for normalized min-sum ldpc decoding," in *2020 IEEE International Conference on Communications Workshops (ICC Workshops)*. IEEE, 2020, pp. 1–6.

[20] M. Helmling, S. Scholl, F. Gensheimer, T. Dietz, K. Kraft, S. Ruzika, and N. Wehn, "Database of channel codes and ml simulation results," www.uni-kl.de/channel-codes, pp. 733–8716, 2019.

[21] J. Dai, K. Tan, Z. Si, K. Niu, M. Chen, H. V. Poor, and S. Cui, "Learning to decode protograph ldpc codes," *Ieee Journal on Selected Areas in Communications*, 2021.

[22] X. Wu, M. Jiang, and C. Zhao, "Decoding optimization for 5g ldpc codes by machine learning," *Ieee Access*, vol. 6, pp. 50 179–50 186, 2018.

[23] L. Wang, S. Chen, J. Nguyen, D. Dariush, and R. Wesel, "Neural-network-optimized degree-specific weights for ldpc minsum decoding," *arXiv preprint arXiv:2107.04221*, 2021.

[24] Y. Kou, S. Lin, and M. P. C. Fossorier, "Low-density parity-check codes based on finite geometries: a rediscovery and new results," *Ieee Transactions on Information Theory*, vol. 47, pp. 2711–2736, 2001.

[25] E. Nachmani, E. Marciano, D. Burshtein, and Y. Be'ery, "Rnn decoding of linear block codes," *arXiv preprint arXiv:1702.07560*, 2017.

[26] T. Richardson and R. Urbanke, *Modern coding theory*. Cambridge university press, 2008.

[27] D. P. Kingma and J. Ba, "Adam: A method for stochastic optimization," *arXiv preprint arXiv:1412.6980*, 2014.

[28] J. Zhang and M. Fossorier, "Shuffled belief propagation decoding," in *Conference Record of the Thirty-Sixth Asilomar Conference on Signals, Systems and Computers*, 2002., vol. 1. IEEE, 2002, pp. 8–15.

[29] L. Lugosch and W. J. Gross, "Learning from the syndrome," in *2018 52nd Asilomar Conference on Signals, Systems, and Computers*. IEEE, 2018, pp. 594–598.